







Electric-quadrupole transition-rate measurement of a highly charged ion in an electron-beam ion trap using pulsed laser excitation from a metastable state

Naoki Kimura ^{1,*}, Priti ², Susumu Kuma ¹, Toshiyuki Azuma ¹ and Nobuyuki Nakamura ³

¹Atomic, Molecular and Optical Physics Laboratory, RIKEN, Saitama 351-0198, Japan

²National Institute for Fusion Science, National Institutes of Natural Sciences, Gifu 509-5292, Japan

³Institute for Laser Science, The University of Electro-Communications, Tokyo 182-8585, Japan

 (Received 13 November 2022; revised 17 January 2023; accepted 24 January 2023; published 9 February 2023)

We present the lifetime measurement of the $(4d_{3/2}^{-1}5s)_{J=2}$ state in Pd-like I^{7+} , which predominantly decays to the $(4d^{10})_{J=0}$ ground state by an electric-quadrupole transition modified by strong spin-orbit mixing. We measure this microsecond-order lifetime in an electron-beam ion trap using pulsed laser excitation from a metastable state which is continuously populated by electron collisions. The measured lifetime provides a new benchmark for relativistic atomic structure calculations with d -state electrons.

DOI: [10.1103/PhysRevA.107.022805](https://doi.org/10.1103/PhysRevA.107.022805)

I. INTRODUCTION

Lifetime measurements of metastable states in highly charged ions (HCIs) have contributed to the verification of theoretical atomic wave functions and the study of relativistic effects on atomic structures, such as spin-orbit coupling in 3P_1 and 3S_1 states [1–27] and hyperfine mixing [28–31]. Recently, lifetimes and transition rates in heavy HCIs with many electrons have become important for various applications. For instance, theoretical transition rates of multiply charged heavy ions have been used for the opacity calculation of astrophysical plasmas for studying early kilonovae [32,33]. The natural width of a metastable state, derived from the lifetime, also provides essential information for discussing its potential for the atomic clock using heavy HCIs [34]. While the bound electrons with the principal quantum number of $n = 4-5$ play an important role in these applications, there are few examples for lifetime measurements of metastable levels involving such electrons in HCIs.

Historically, heavy-ion storage ring experiments have pioneered measurements of lifetimes in HCIs greater than milliseconds [35]. Electron-beam ion traps (EBITs) combined with an electron-beam-off technique under strong magnetic fields are also powerful tools for measuring metastable state lifetimes [36]. Developments of laser spectroscopy of HCIs [37–43] also offer new possibilities for lifetime measurements. State-selective lifetime measurement schemes using resonant laser spectroscopy [37,41] and quantum logic laser spectroscopy [43] have been demonstrated by employing the millisecond-order visible or ultraviolet magnetic-dipole (M1) transition.

In this paper, we study the microsecond-order lifetime of $(4d_{3/2}^{-1}5s)_{J=2}$ in Pd-like I^{7+} . Figure 1 shows the energy level structure of I^{7+} calculated with the Flexible Atomic Code (FAC 1.1.5) [44]. The term $(4d_{3/2}^{-1}5s)_{J=2}$ of the fifth-lowest level in

I^{7+} is given by FAC based on the jj -coupling scheme. The National Institute of Standards and Technology (NIST) database [45] gives a leading term of 1D_2 in the LS -coupling scheme with a percentage of 63%. The main decay path of this state is to the ground $(4d^{10})_{J=0}$ (1S_0) via a spin-allowed electric-quadrupole (E2) transition with extreme ultraviolet (EUV) emission; its lifetime ($\sim 4 \mu\text{s}$) substantially reflects significant mixing with the 3D_2 level whose decay is spin forbidden. While the experimental lifetime of this state has the potential to be a benchmark for developing reliable atomic structure calculations of relativistic many-electron systems with d electrons, it is generally difficult to measure such short lifetimes. Although the conventional EBIT technique has successfully

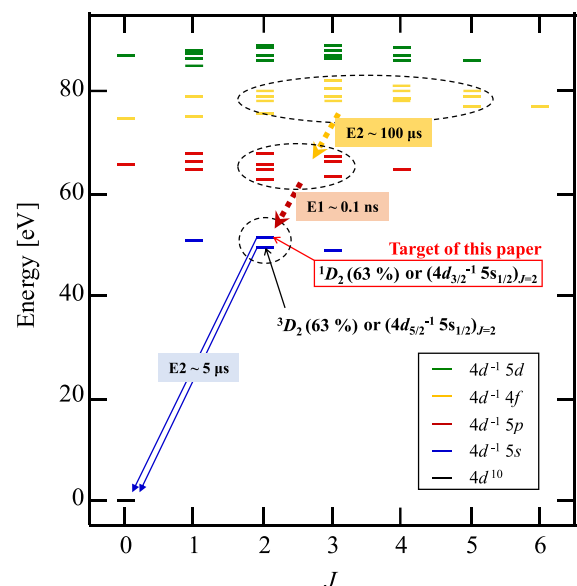


FIG. 1. Energy levels in Pd-like I^{7+} calculated with FAC [44]. The transition of interest, $(4d^{10})_{J=0}-(4d_{3/2}^{-1}5s)_{J=2}$, and the cascade processes contributing to the repopulation of $(4d_{3/2}^{-1}5s)_{J=2}$ are also shown.

*naoki.kimura@riken.jp

demonstrated microsecond-order lifetime measurements of He-like ions [27] and Ne-like ions [46], it is not applicable to all metastable states with a microsecond-order lifetime. In the present $(4d_{3/2}^{-1}5s)_{J=2}$ state, repopulation effects caused by cascade processes slower than the transition of interest obscure the radiative decay in the microsecond-order time range, as shown in Fig. 1. Additionally, in the conventional EBIT technique, possible loss of trapped ions due to changes in the trap condition when turning off the electron beam should be carefully taken into account [27]. These experimental difficulties are not specific to the present transition but are common challenges in lifetime measurements of HCIs on time scales shorter than 1 ms [47–49]. Here we demonstrate a lifetime measurement scheme offering a new solution to these experimental difficulties.

II. EXPERIMENT

Figure 2 shows the present experimental scheme with the level structure of I^{7+} . The experiment was performed by applying the technique of time-resolved laser spectroscopy with the aid of excitation processes in the EBIT, first proposed by Ralchenko [50] and recently demonstrated by our group [51]. This laser spectroscopy has extended the cw-laser-induced fluorescence spectroscopy of a $2s$ - $2p$ transition of H-like ions in an EBIT [52–55], which was demonstrated by Hosaka *et al.* [40]. We record the time-resolved laser-induced fluorescence (LIF) signal from I^{7+} ions prepared in a compact electron-beam ion trap (CoBIT) [56]. I^{7+} has four low-lying metastable fine-structure levels in the first excited electron configuration $4d^{-1}5s$. In the EBIT, this configuration is continuously populated through collisional and radiative processes. The population rate for each fine-structure level was estimated to be $\sim 160 \text{ s}^{-1}$ by theoretical calculations based on collisional-radiative modeling [57]. The lowest metastable $(4d_{5/2}^{-1}5s)_{J=3}$ level possesses the large population in the EBIT ($>10\%$) because the radiative depopulation rate is at least 10^3 times slower than the population rate for every hyperfine level since it slowly decays to the ground $(4d^{10})_{J=0}$ through magnetic-octupole (M3) and hyperfine-mixing E2 transitions. We performed wavelength- and time-resolved observation of the E2 $(4d_{3/2}^{-1}5s)_{J=2} \rightarrow (4d^{10})_{J=0}$ emission ($\lambda = 25.2 \text{ nm}$ in vacuum) induced by pulsed laser excitation of the M1 transition $(4d_{5/2}^{-1}5s)_{J=3} \rightarrow (4d_{3/2}^{-1}5s)_{J=2}$ ($\lambda = 566.94 \text{ nm}$ in air) from the highly populated long-lived level. It is noted that to observe the LIF signal, the number of pulsed-laser-excited ions should be larger than the time-independent component of the $(4d_{3/2}^{-1}5s)_{J=2}$ state population pumped by collisional and radiative processes in the EBIT. The population of $(4d_{5/2}^{-1}5s)_{J=3}$ is more than a thousand times larger than $(4d_{3/2}^{-1}5s)_{J=2}$. This fact satisfies the condition for the sufficient population transfer via the M1 transition during the nanosecond-order laser pulse. The state-selective observation of the transition decay dynamics, triggered by the pulsed laser excitation, allows for accurate measurement by eliminating the systematic uncertainties associated with the cascade processes from upper states. The number of trapped ions was successfully maintained during the observation of the decay profile by the laser excitation without any change in the trap condition.

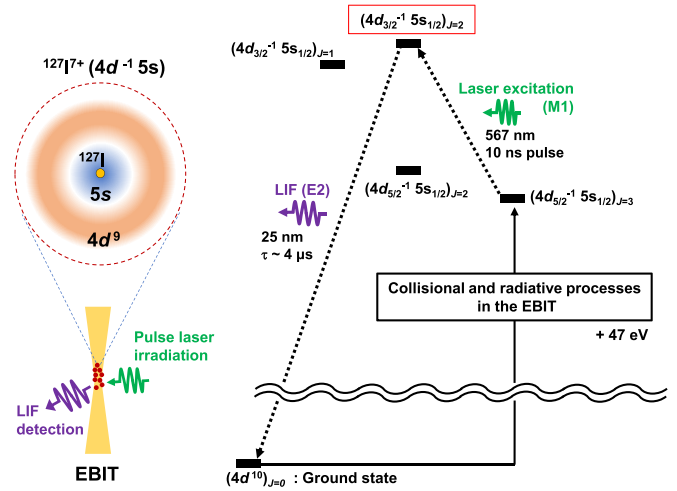


FIG. 2. Experimental scheme with the energy diagram of I^{7+} .

The details of CoBIT have been described in a previous paper [56]. Our recent article [51] also provides a detailed description of the present LIF experimental setup. Briefly, CoBIT consists of a magnetically compressed electron beam through three successive cylindrical drift-tube electrodes (DT1, 2, and 3) forming the trap potential. I^{7+} ions were prepared from CH_3I vapor by successive ionization processes in the trap region [57]. The typical electron-beam energy, electron-beam current, and drift-tube potential are 105 eV, 2 mA, and 50 V, respectively. To excite the M1 transition, we used a wavelength-tunable pulsed dye laser (Sirah Cobra-Stretch with the dual 3000 lines/mm grating option, Exciton Rhodamine 6G/Ethanol dye solution pumped by Cutting Edge Optics Gigashot, maximum 20 mJ/pulse at 567 nm). The typical time width of the pulsed dye laser is 10 ns. The laser emission timing was triggered by a function generator signal with a 100 Hz repetition rate. We performed the selective observation of the E2 $(4d_{3/2}^{-1}5s)_{J=2} \rightarrow (4d^{10})_{J=0}$ emission using a time-resolving extreme ultraviolet (EUV) spectrometer consisting of an aberration-corrected concave grating (Hitachi 001-0660) and a position-sensitive detector (PSD; Quantar Technology, model 3391) based on a position-sensitive microchannel plate (MCP) [58,59]. The timing of the observed E2 emission signal with respect to the laser excitation pulse was recorded with a multichannel scaler (MCS; TechnoAP, model APG7400A). The time resolution of this measurement system is 40 ns limited by the minimum bin size of the MCS. The pulsed-laser-excited component predominates over the time-independent population of $(4d_{5/2}^{-1}5s)_{J=2}$ through the collisional and radiative processes within the microsecond-order time range window. However, it is noted that the estimated average excitation rate, $\sim 1 \text{ s}^{-1}$, by the pulsed laser with a 100 Hz repetition rate is much slower than the population rate, $\sim 160 \text{ s}^{-1}$. Thus the LIF was persistently emitted without depletion of the population in the initial level $(4d_{5/2}^{-1}5s)_{J=3}$.

III. RESULTS AND DISCUSSION

Figure 3 shows the measured LIF decay profile. The accumulation time is 53 h. We successfully observed the decay

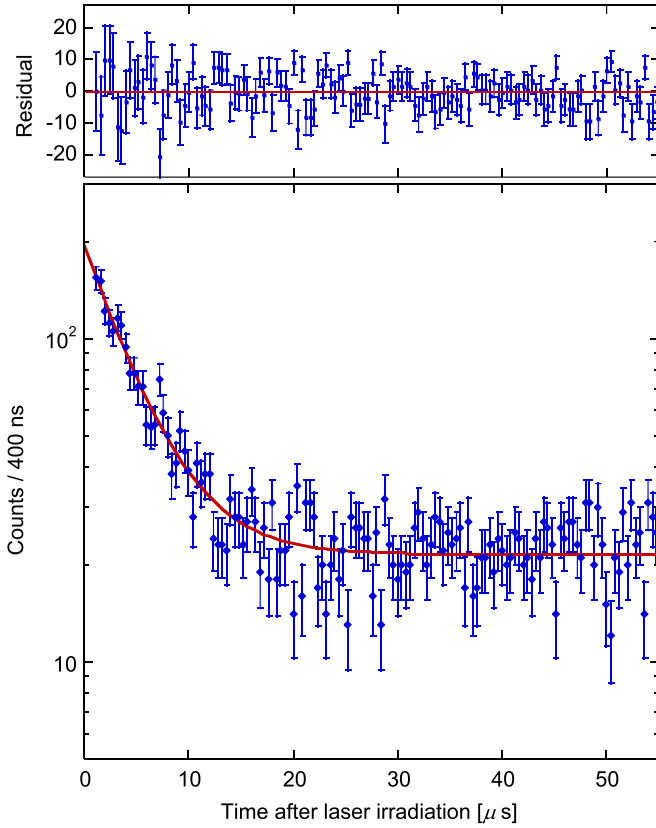


FIG. 3. Bottom: Experimentally observed LIF decay profile. The red line represents the fitting result. Top: Residuals of the experimental plots from the fitting line. Error bars reflect Poisson counting statistics.

profile from the $(4d_{3/2}^{-1}5s)_{J=2}$ state and were able to disentangle it from cascade contributions by using the pulsed laser excitation. The experimental plots converged to the background level around 50 μs after laser excitation. The background component originates from the continuous E2 emission due to electron collisions and radiative processes in the EBIT. A single exponential function with a constant background was fitted to the observed decay profile, and the transition probability from the $(4d_{3/2}^{-1}5s)_{J=2}$ state was determined to be $2.32 \times 10^5 \text{ s}^{-1}$ with a statistical uncertainty of $\pm 0.07 \times 10^5 \text{ s}^{-1}$. We also evaluated the systematic uncertainties. Collisional processes with electrons and residual neutral particles in the EBIT enhance the decay of the laser-excited state $(4d_{3/2}^{-1}5s)_{J=2}$, contributing to the uncertainty. Using FAC [44], we theoretically estimated the total excitation and deexcitation rate of the $(4d_{3/2}^{-1}5s)_{J=2}$ state by electron collisions in the present EBIT condition to be $9 \times 10^2 \text{ s}^{-1}$ [51]. The collision rate with residual gas ($\sim 10^{-9} \text{ Pa}$) is less than the 10^1 s^{-1} which was estimated with Müller and Salzborn's empirical formula [60]. In addition, we evaluated instrumental systematic uncertainties [e.g., the laser emission timing jitter ($< 1 \text{ ns}$) and the record timing fluctuation due to the PSD ($< 1 \text{ ns}$)] and found them to be less than 10^2 s^{-1} . We finally adopted a total systematic uncertainty of $1 \times 10^3 \text{ s}^{-1}$. The resulting transition probability and corresponding lifetime are

summarized in Table I, along with the theoretical calculations discussed below.

The $(4d_{3/2}^{-1}5s)_{J=2}$ metastable state has one E2 transition decay channel to the ground state $(4d^{10})_{J=0}$ and three M1 transition decay channels to $(4d_{3/2}^{-1}5s)_{J=1}$, $(4d_{5/2}^{-1}5s)_{J=2}$, and $(4d_{5/2}^{-1}5s)_{J=3}$. Since the $(4d_{3/2}^{-1}5s)_{J=2}$ fine-structure level possesses hyperfine structure, we theoretically evaluated the hyperfine-state dependence of the lifetime using the HFSZEMAN95 package [61,62] and found that the hyperfine-mixing effect is negligibly small [51]. Therefore, in the following, we discuss the theoretical lifetime of the $(4d_{3/2}^{-1}5s)_{J=2}$ fine-structure level without hyperfine-state dependence. The transition probabilities A_{E2} for the E2 transition and $A_{M1,J=1-3}$ for the M1 transitions (in s^{-1}) are given by the line strengths between $(4d_{3/2}^{-1}5s)_{J=2}$ and the lower fine-structure levels as follows [63]:

$$A_{E2} = \frac{1.11995 \times 10^{18}}{\lambda^5 (2J+1)} S_{E2}, \quad (1)$$

$$A_{M1} = \frac{2.69735 \times 10^{13}}{\lambda^3 (2J+1)} S_{M1}. \quad (2)$$

Here, λ is the transition wavelength (in angstroms). The line strengths S_{E2} and S_{M1} (in atomic units) are obtained by the sum of the squares of the reduced matrix element with electric-quadrupole (E2) and magnetic-dipole (M1) operators, respectively. For the S_{E2} calculation, we employed the Coulomb and Babushkin gauges [64], which correspond to the velocity and length gauges, respectively. To obtain the reduced matrix element, we used the atomic state wave functions calculated in our previous paper [51]. Briefly, the wave-function calculation is based on the multiconfiguration Dirac-Fock (MCDF) method combined with the relativistic configuration interaction (RCI) approach using GRASP2K2018 [65]. Various correlation effects are taken into account by including the configurational state functions (CSFs) generated from single-double (SD) excitation from the reference configuration (DF) to the active space (AS) defined as follows:

$$\text{DF} = \{3s^2 3p^6 4s^2 4p^6 4d^{10}, 3s^2 3p^6 4s^2 4p^6 4d^9 5s^1\},$$

$$\text{AS1} = \text{DF} + \{5p, 5d, 5f, 5g\},$$

$$\text{AS2} = \text{AS1} + \{6s, 6p, 6d, 6f, 6g, 6h\},$$

$$\text{AS3} = \text{AS2} + \{7s, 7p, 7d, 7f, 7g, 7h\},$$

$$\text{AS4} = \text{AS3} + \{8s, 8p, 8d, 8f, 8g, 8h\}.$$

In the present calculation, all electrons are categorized into two types: Electrons in $4d$ and $5s$ orbitals are taken as valence electrons and in other inner orbitals as core electrons. The correlation was thus taken as the interaction between valence-valence (VV), core-valence (CV), and core-core (CC) electrons. This active space treatment led to 3 300 000 jj -coupled configurations in the set AS4. The Breit interaction, i.e., transverse photon interaction in the low-frequency limit, and quantum electrodynamics (QED) effects from self-energy correction (SE) and vacuum polarization (VP) were also included in subsequent RCI calculations.

The theoretical results summarized in Table I employed the full active space set AS4 including the RCI correction. The calculated major terms for the LS composition in this

TABLE I. Summary of the experimental and theoretical lifetime τ with calculated individual transition probabilities. The theoretical values were calculated by employing the active space set AS4 and include the RCI correction.

	Decay channel	Experiment	Theory	
			Coulomb gauge	Babushkin gauge
$A_{E2} (s^{-1})$	$(4d^{10})_{J=0}$		2.32×10^5	2.19×10^5
$A_{M1,J=3} (s^{-1})$	$(4d_{3/2}^{-1}5s)_{J=3}$			4.95×10^1
$A_{M1,J=2} (s^{-1})$	$(4d_{3/2}^{-1}5s)_{J=2}$			3.06×10^0
$A_{M1,J=1} (s^{-1})$	$(4d_{3/2}^{-1}5s)_{J=1}$			3.52×10^{-1}
$A_{\text{total}} (s^{-1})$		$2.32(\pm 0.07_{\text{stat}} \pm 0.01_{\text{sys}}) \times 10^5$	2.32×10^5	2.19×10^5
$\tau (\mu s)$		$4.31(\pm 0.14_{\text{stat}} \pm 0.02_{\text{sys}})$	4.31	4.57

metastable state are 1D_2 (61%) and 3D_2 (34%). As shown in the calculation results, the $(4d_{3/2}^{-1}5s)_{J=2} - (4d^{10})_{J=0}$ transition accounts for 99.98% of the decay processes from $(4d_{3/2}^{-1}5s)_{J=2}$. Since the contribution of other decay channels is two orders smaller than the experimental uncertainty, the present experiment can verify the theoretical calculation of the E2 transition lifetime. Theoretical values from both the Coulomb and Babushkin gauges show a good agreement with the experimental result within 2σ . The uncertainties of the calculated transition rates of E1-allowed transitions are generally evaluated by the difference between the different gauge calculations [66]. When we adopt this convention, the theoretical uncertainty is about 5%. In Table II, the individual contributions of VV, CV, and CC correlations, as well as the RCI correction in the E2 transition-rate calculation, are shown. In contrast to the importance of electron correlations, the Breit and QED effects calculated by the RCI calculation are small.

From the present transition probability of $2.32(\pm 0.08) \times 10^5 s^{-1}$ along with the transition wavelength of $252.7(\pm 0.2) \text{ \AA}$ reported in our previous paper [57], we determined the experimental line strength of the E2 transition (S_{E2}) to be $1.07(\pm 0.04)$. Figure 4 shows the active space set dependence of the theoretical line strength of the E2 transition along with the experimental result. In the full active space set calculation (AS4), the theoretical values between the two different gauges are close to each other, indicating a convergence behavior around the experimental value. Although we could not conclude which calculation is more accurate due to the present experimental uncertainty, different active space set dependencies for the Coulomb and

Babushkin gauge calculations were found. The Coulomb gauge calculation results show a strong active space set dependence, in contrast to the nearly constant behavior of the Babushkin gauge calculations. This behavior is the opposite of the recently reported gauge dependence in E1 transitions regarding Rydberg series [67] and may be caused by the present s - d transition property between the contracted electron clouds of HClIs. Since the Coulomb gauge is generally sensitive to the inner part of the wave function, it may emphatically reflect the calculation accuracy of the wave function around the inner part. In MCDF calculations, constructing a complete orbital basis set and including the RCI correlations as accurately as possible are necessary to reach the convergence. In the future, there is a possibility to verify the convergence by including further active spaces ($n > 8$) and the configurations from triple excitations, which we have not considered in the present calculations due to computational restrictions. The systematic transition-rate calculation using extreme gauges other than the Coulomb and Babushkin gauges, which has been recently performed for verifying theoretical atomic wave functions, is also possible to contribute to judging the convergence [68,69]. These developments of theoretical calculation with the benchmark given by the experimental lifetime measurement

TABLE II. Theoretical transition probabilities of the E2 transition $(4d^{10})_{J=0} - (4d_{3/2}^{-1}5s)_{J=2}$ with separated correlations. Calculations were performed with the active space set AS4.

Contribution	Coulomb gauge (s^{-1})	Babushkin gauge (s^{-1})
DF	2.27×10^5	2.05×10^5
+VV	-0.07×10^5	$+0.30 \times 10^5$
+CV	$+0.15 \times 10^5$	-0.12×10^5
+CC	-0.04×10^5	-0.03×10^5
+RCI	$+0.01 \times 10^5$	$+0.00 \times 10^5$
MCDF +RCI	2.32×10^5	2.19×10^5

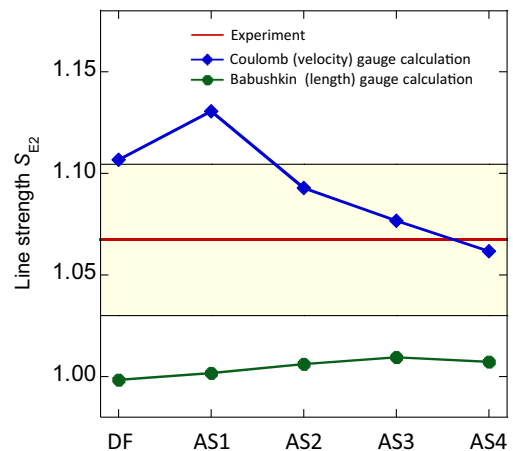


FIG. 4. Active space set dependence of the E2 transition line strength (in atomic units) in the MCDF calculation without the RCI correction. The thin black lines represent the experimental uncertainty (1σ).

are worthwhile because atomic wave functions calculated by an incomplete basis set, even if they provide accurate energy levels, do not ensure accuracy in other properties such as transition rates [67].

IV. CONCLUSION

We demonstrated a lifetime measurement scheme solving the experimental difficulties caused by repopulation effects due to cascade contributions from upper metastable levels. By time-resolved laser-induced fluorescence spectroscopy between the metastable fine-structure levels of $(4d_{5/2}^{-1}5s)_{J=3}$ and $(4d_{3/2}^{-1}5s)_{J=2}$ in Pd-like I^{7+} , the lifetime of the E2 transition $(4d^{10})_{J=0}-(4d_{3/2}^{-1}5s)_{J=2}$ was successfully measured with a 3% uncertainty. The experimental lifetime involving spin-orbit coupling with d electrons provides a crucial benchmark for atomic structure calculations for many-electron HCIs. We compared the measured lifetime with theoretical calculations

based on the multiconfiguration Dirac-Fock method combined with the relativistic configuration-interaction approach and found a good agreement. Additionally, we studied the convergence behavior in active space set dependencies of Coulomb and Babushkin gauge calculations. The present investigation adds the test of the E2 transition to recent theoretical discussions on the gauge dependence of computational convergence properties [67–70].

ACKNOWLEDGMENTS

We appreciate the fruitful discussion with Dr. Marianna Safronova and Dr. Daiji Kato. We would like to thank Dr. Haruka Tanji-Suzuki for providing an optical table. We also thank Dr. Kiattichart Chartkunchand for critical reading of the manuscript. This work was supported by the RIKEN Pioneering Projects and by JSPS KAKENHI Grants No. 20K20110 and No. 22K13990.

-
- [1] H. Gould, R. Marrus, and R. W. Schmieder, *Phys. Rev. Lett.* **31**, 504 (1973).
- [2] C. L. Cocke, B. Curnutte, and R. Randall, *Phys. Rev. Lett.* **31**, 507 (1973).
- [3] J. A. Bednar, C. L. Cocke, B. Curnutte, and R. Randall, *Phys. Rev. A* **11**, 460 (1975).
- [4] D. D. Dietrich, J. A. Leavitt, S. Bashkin, J. G. Conway, H. Gould, D. MacDonald, R. Marrus, B. M. Johnson, and D. J. Pegg, *Phys. Rev. A* **18**, 208 (1978).
- [5] D. D. Dietrich, J. A. Leavitt, H. Gould, and R. Marrus, *Phys. Rev. A* **22**, 1109 (1980).
- [6] R. Marrus, P. Charles, P. Indelicato, L. de Billy, C. Tazi, J.-P. Briand, A. Simionovici, D. D. Dietrich, F. Bosch, and D. Liesen, *Phys. Rev. A* **39**, 3725(R) (1989).
- [7] G. Möller, E. Träbert, V. Lodwig, C. Wagner, P. H. Heckmann, J. H. Blanke, A. E. Livingston, and P. H. Mokler, *Z. Phys. D: At. Mol. Clusters* **11**, 333 (1989).
- [8] R. W. Dunford, D. A. Church, C. J. Liu, H. G. Berry, M. L. A. Raphaelian, M. Hass, and L. J. Curtis, *Phys. Rev. A* **41**, 4109(R) (1990).
- [9] M. Westerlind, L. Engström, P. Bengtsson, and L. J. Curtis, *Phys. Rev. A* **45**, 6198 (1992).
- [10] B. J. Wargelin, P. Beiersdorfer, and S. M. Kahn, *Phys. Rev. Lett.* **71**, 2196 (1993).
- [11] V. H. S. Kwong, Z. Fang, T. T. Gibbons, W. H. Parkinson, and P. L. Smith, *Astrophys. J.* **411**, 431 (1993).
- [12] H. T. Schmidt, P. Forck, M. Grieser, D. Habs, J. Kenntner, G. Miersch, R. Repnow, U. Schramm, T. Schüssler, D. Schwalm, and A. Wolf, *Phys. Rev. Lett.* **72**, 1616 (1994).
- [13] S. Cheng, R. W. Dunford, C. J. Liu, B. J. Zabransky, A. E. Livingston, and L. J. Curtis, *Phys. Rev. A* **49**, 2347 (1994).
- [14] J. Doerfert, E. Träbert, J. Granzow, A. Wolf, J. Kenntner, D. Habs, M. Grieser, T. Schüssler, U. Schramm, and P. Forck, *Nucl. Instrum. Methods Phys. Res., Sect. B* **98**, 53 (1995).
- [15] L. J. Curtis, S. T. Maniak, R. W. Ghrist, R. E. Irving, D. G. Ellis, M. Henderson, M. H. Kacher, E. Träbert, J. Granzow, P. Bengtsson, and L. Engström, *Phys. Rev. A* **51**, 4575 (1995).
- [16] G. S. Stefanelli, P. Beiersdorfer, V. Decaux, and K. Widmann, *Phys. Rev. A* **52**, 3651 (1995).
- [17] P. Beiersdorfer, L. Schweikhard, J. R. Crespo López-Urrutia, and K. Widmann, *Rev. Sci. Instrum.* **67**, 3818 (1996).
- [18] E. Träbert, *Phys. Scr.* **53**, 167 (1996).
- [19] J. Doerfert, E. Träbert, A. Wolf, D. Schwalm, and O. Uwira, *Phys. Rev. Lett.* **78**, 4355 (1997).
- [20] J. R. Crespo López-Urrutia, P. Beiersdorfer, D. W. Savin, and K. Widmann, *Phys. Rev. A* **58**, 238 (1998).
- [21] E. Träbert, A. Wolf, J. Linkemann, and X. Tordoir, *J. Phys. B: At. Mol. Opt. Phys.* **32**, 537 (1999).
- [22] E. Träbert, P. Beiersdorfer, G. V. Brown, A. J. Smith, S. B. Utter, M. F. Gu, and D. W. Savin, *Phys. Rev. A* **60**, 2034 (1999).
- [23] P. A. Neill, E. Träbert, P. Beiersdorfer, G. V. Brown, C. L. Harris, S. B. Utter, and K. L. Wong, *Phys. Scr.* **62**, 141 (2000).
- [24] E. Träbert, A. Wolf, and G. Gwinner, *Phys. Lett. A* **295**, 44 (2002).
- [25] E. Träbert, G. Gwinner, E. J. Knystautas, and A. Wolf, *Can. J. Phys.* **81**, 941 (2003).
- [26] E. Träbert, E. J. Knystautas, G. Saathoff, and A. Wolf, *J. Phys. B: At. Mol. Opt. Phys.* **38**, 2395 (2005).
- [27] J. R. Crespo López-Urrutia, P. Beiersdorfer, and K. Widmann, *Phys. Rev. A* **74**, 012507 (2006).
- [28] E. Träbert, P. Beiersdorfer, G. V. Brown, K. Boyce, R. L. Kelley, C. A. Kilbourne, F. S. Porter, and A. Szymkowiak, *Phys. Rev. A* **73**, 022508 (2006).
- [29] E. Träbert, P. Beiersdorfer, and G. V. Brown, *Phys. Rev. Lett.* **98**, 263001 (2007).
- [30] S. Schippers, E. W. Schmidt, D. Bernhardt, D. Yu, A. Müller, M. Lestinsky, D. A. Orlov, M. Grieser, R. Repnow, and A. Wolf, *Phys. Rev. Lett.* **98**, 033001 (2007).
- [31] S. Schippers, D. Bernhardt, A. Müller, M. Lestinsky, M. Hahn, O. Novotný, D. W. Savin, M. Grieser, C. Krantz, R. Repnow, and A. Wolf, *Phys. Rev. A* **85**, 012513 (2012).
- [32] S. Banerjee, M. Tanaka, K. Kawaguchi, D. Kato, and G. Gaigalas, *Astrophys. J.* **901**, 29 (2020).

- [33] S. Banerjee, M. Tanaka, D. Kato, G. Gaigalas, K. Kawaguchi, and N. Domoto, *Astrophys. J.* **934**, 117 (2022).
- [34] M. G. Kozlov, M. S. Safronova, J. R. Crespo López-Urrutia, and P. O. Schmidt, *Rev. Mod. Phys.* **90**, 045005 (2018).
- [35] E. Träbert, *Phys. Scr.* **2002**, 88 (2002).
- [36] E. Träbert, *J. Phys.: Conf. Ser.* **72**, 012006 (2007).
- [37] I. Klaft, S. Borneis, T. Engel, B. Fricke, R. Grieser, G. Huber, T. Kühl, D. Marx, R. Neumann, S. Schröder, P. Seelig, and L. Völker, *Phys. Rev. Lett.* **73**, 2425 (1994).
- [38] E. G. Myers, P. Kuske, H. J. Andrä, I. A. Armour, N. A. Jelley, H. A. Klein, J. D. Silver, and E. Träbert, *Phys. Rev. Lett.* **47**, 87 (1981).
- [39] E. G. Myers, H. S. Margolis, J. K. Thompson, M. A. Farmer, J. D. Silver, and M. R. Tarbutt, *Phys. Rev. Lett.* **82**, 4200 (1999).
- [40] K. Hosaka, D. N. Crosby, K. Gaarde-Widdowson, C. J. Smith, J. D. Silver, T. Kinugawa, S. Ohtani, and E. G. Myers, *Phys. Rev. A* **69**, 011802(R) (2004).
- [41] V. Mäckel, R. Klawitter, G. Brenner, J. R. Crespo López-Urrutia, and J. Ullrich, *Phys. Rev. Lett.* **107**, 143002 (2011).
- [42] K. Schnorr, V. Mäckel, N. S. Oreshkina, S. Augustin, F. Brunner, Z. Harman, J. Ullrich, and J. R. Crespo López-Urrutia, *Astrophys. J.* **776**, 121 (2013).
- [43] P. Micke, T. Leopold, S. A. King, E. Benkler, L. J. Spieß, L. Schmöger, M. Schwarz, J. R. Crespo López-Urrutia, and P. O. Schmidt, *Nature (London)* **578**, 60 (2020).
- [44] M. F. Gu, *Can. J. Phys.* **86**, 675 (2008).
- [45] A. Kramida, Y. Ralchenko, J. Reader, and NIST ASD Team, NIST atomic spectra database (version 5.9), 2021, <http://physics.nist.gov/asd>.
- [46] J. R. Crespo López-Urrutia and P. Beiersdorfer, *Astrophys. J.* **721**, 576 (2010).
- [47] E. Träbert, *J. Phys. B: At. Mol. Opt. Phys.* **43**, 074034 (2010).
- [48] E. Träbert, *Phys. Scr.* **79**, 068101 (2009).
- [49] E. Träbert, *Atoms* **10**, 114 (2022).
- [50] Y. Ralchenko, *Nucl. Instrum. Methods Phys. Res., Sect. B* **408**, 38 (2017).
- [51] N. Kimura, Priti, Y. Kono, P. Pipatpakorn, K. Soutome, N. Numadate, S. Kuma, T. Azuma, and N. Nakamura, *Commun. Phys.* **6**, 8 (2023).
- [52] H. S. Margolis, P. D. Groves, J. D. Silver, and M. A. Levine, *Hyperfine Interact.* **99**, 169 (1996).
- [53] T. V. Back, P. D. Groves, H. S. Margolis, P. K. Oxley, and J. S. Silver, *Phys. Scr.* **1997**, 62 (1997).
- [54] T. V. Back, H. S. Margolis, P. K. Oxley, J. D. Silver, and E. G. Myers, *Hyperfine Interact.* **114**, 203 (1998).
- [55] H. A. Klein, H. S. Margolis, J. L. Flowers, K. Gaarde-Widdowson, K. Hosaka, J. D. Silver, M. R. Tarbutt, S. Ohtani, and D. J. E. Knight, *Lect. Notes Phys.* **570**, 664 (2001).
- [56] N. Nakamura, H. Kikuchi, H. A. Sakaue, and T. Watanabe, *Rev. Sci. Instrum.* **79**, 063104 (2008).
- [57] N. Kimura, R. Kodama, Priti, N. Numadate, K. Suzuki, M. Monobe, and N. Nakamura, *Phys. Rev. A* **102**, 032807 (2020).
- [58] H. Ohashi, J. Yatsurugi, H. A. Sakaue, and N. Nakamura, *Rev. Sci. Instrum.* **82**, 083103 (2011).
- [59] T. Tsuda, E. Shimizu, S. Ali, H. A. Sakaue, D. Kato, I. Murakami, H. Hara, T. Watanabe, and N. Nakamura, *Astrophys. J.* **851**, 82 (2017).
- [60] A. Müller and E. Salzborn, *Phys. Lett. A* **62**, 391 (1977).
- [61] M. Andersson and P. Jönsson, *Comput. Phys. Commun.* **178**, 156 (2008).
- [62] W. Li, J. Grumer, T. Brage, and P. Jönsson, *Comput. Phys. Commun.* **253**, 107211 (2020).
- [63] R. D. Cowan, *The Theory of Atomic Structure and Spectra* (University of California Press, Berkeley, 1981).
- [64] I. P. Grant, *J. Phys. B: At. Mol. Phys.* **7**, 1458 (1974).
- [65] C. Froese Fischer, G. Gaigalas, P. Jönsson, and J. Bieroń, *Comput. Phys. Commun.* **237**, 184 (2019).
- [66] C. Froese Fischer, G. Tachiev, and A. Irimia, *At. Data Nucl. Data Tables* **92**, 607 (2006).
- [67] A. Papoulia, J. Ekman, G. Gaigalas, M. Godefroid, S. Gustafsson, H. Hartman, W. Li, L. Radžiūtė, P. Rynkun, S. Schiffmann, K. Wang, and P. Jönsson, *Atoms* **7**, 106 (2019).
- [68] G. Gaigalas, P. Rynkun, S. Banerjee, M. Tanaka, D. Kato, and L. Radžiūtė, *Mon. Not. R. Astron. Soc.* **517**, 281 (2022).
- [69] P. Rynkun, S. Banerjee, G. Gaigalas, M. Tanaka, L. Radžiūtė, and D. Kato, *Astron. Astrophys.* **658**, A82 (2022).
- [70] A. Pehlivan Rhodin, H. Hartman, H. Nilsson, and P. Jönsson, *Astron. Astrophys.* **598**, A102 (2017).